Paper ID ILASS08-11-2

INFLUENCE OF FLAME ON PRIMARY ATOMIZATION IN OXY – LIQUID FUEL FLAMES

B. Leroux*, X. Paubel*, N. Darabiha° and F. Lacas°

* Air Liquide, Centre de Recherche Claude Delorme, Les Loges en Josas – BP 126
78350 Jouy en Josas, France. Phone : + 33 1 39 07 63 38 Fax: + 33 1 39 07 61 13
bertrand.leroux@airliquide.com
° Laboratoire EM2C - C.N.R.S., Ecole Centrale Paris - Grande Voie des Vignes
92295 Châtenay-Malabry, France

ABSTRACT
The influence of flame on primary atomization in oxy- liquid ethanol flames is experimentally investigated by using a coaxial air-assisted injector positioned in a vertical combustion chamber. Flame structure is observed through CH emission, liquid phase by laser tomography.
Classifying atomizing modes in presence of flame shows that momentum flux ratio J and gas Reynolds number Re_g are still relevant parameters; however the limits defined in cold spray conditions between the various regimes do not seem valid anymore. In particular the values of J and Re_g for which atomization is efficient enough are much higher in presence of flame. The conclusions are the same for break-up length: in presence of flame, break-up length is two to six times as important as in cold spray conditions.
An analytical model is then proposed, based on the idea that this is not annular gas flow which causes primary atomization but a mixture of burnt gases and vaporized ethanol. New scales are then chosen: for length scale, the inner tube thickness and for velocity scale, the average velocity of the burnt gases – vaporized ethanol mixture. Thanks to this model, it is possible to assess an analytical break-up length close to experimental data.

INTRODUCTION

Oxy- liquid fuel combustion has found many applications within the last years, especially in glass or metallurgy industries. The main purpose is to increase the combustion temperature and to enhance subsequently thermal transfer. A second purpose lies in the fact that, by reducing the nitrogen content in the oxidizer, nitrogen oxides (NOx) production is significantly reduced. A new and promising application of oxy- combustion is to increase the CO2 concentration in burnt gases and to improve the efficiency of CO2 capturing processes to reduce greenhouse effect gases emission.

One particularity of oxy combustion is the reduction of reaction time since laminar flame speed is significantly higher (about five to ten times, see [1]). In case of liquid fuels, flame geometry is then driven by droplets vaporization and atomization quality. Consequently characterizing spray properties of the used injectors is particularly relevant for oxy burner design and operation.

This has motivated studies led by [2] on coaxial air-assisted atomizers in cold spray conditions. Due to their easy built configuration and good atomization performances, these injectors are indeed widely used in many industrial applications especially in oxy combustion. In this type of atomizing device, a liquid jet flowing at a velocity U_l is exposed to an annular gaseous flow, the high speed of which is noted U_g. A classification of atomization regimes has been proposed by [2] for which the determining parameters are the momentum flux ratio J and gas Reynolds number Re_g, with:

$$J = \frac{\rho_g U_g^{\ 2}}{\rho_l U_l^{\ 2}}, \qquad (1)$$

$$\mathrm{Re}_g = \frac{\rho_g U_g (D_{go} - D_{gi})}{\mu_g}, \qquad (2)$$

where ρ_g and ρ_l stand for gas and liquid densities, μ_g dynamic viscosity of gas and D_{go}-D_{gi} the diameter of annular gas flow. A criterion existence based on the two numbers has been also proposed for Rayleigh and superpulsating modes. When $J < J_r$, atomization mode remains Rayleigh type whereas when $J > J_{sp}$, disintegration mode becomes superpulsating. J_r and J_{sp} depend on Re_g as follows:

$$J_r = \frac{7\,10^6}{\mathrm{Re}_g^{1.9}}, \qquad (3)$$

$$J_{sp} = \frac{2\,10^5}{\mathrm{Re}_g^{1.1}}. \qquad (4)$$

For $J_r < J < J_{sp}$, atomization mode is membrane and fiber type. These results are consistent with other observations found in literature (see for instance [3] and [4])

Another result put into evidence by [2] has been the influence of momentum flux ratio J on break-up length L_b according to the following relation:

$$\frac{L_b}{D_l} = \frac{10}{J^{0.33}}. \qquad (5)$$

In air combustion, the characterization of spray in cold conditions would have been enough since atomization and combustion are uncoupled. Flame is indeed stabilized at a certain distance of the injection and droplets are formed

before the combustion zone. Flame influence is usually limited to droplets size evolution in the dilute zone as mentioned by [5], [6] or [7]. When comparing spray properties between "cold" and "hot" conditions, these authors emphasize essentially the increase of Sauter Mean Diameter (SMD) in presence of flame, phenomenon due to the vaporization of smallest droplets.

But for oxy firing case, flame is sometimes stabilized on burner tip as shown by [8]. In this case, liquid phase vaporization and reaction begin at the same time as primary atomization: droplets formation is likely to be strongly influenced by flame presence.

Consequently the present work is aimed at determining if correlations put into evidence by [2] are still valid in two phase oxy combustion conditions. For that, we have performed a small scale experimental study, using liquid ethanol as fuel. Ethanol is indeed easy to handle and it produces a limited amount of soot. Due to the high temperature level in oxy-fuel combustion, soot emissions might be a serious problem in the use of optical diagnostics.

After a description of the experimental set-up and diagnostic techniques we used, we show the modification of atomizing modes and break-up length in presence of flame. An analytical model is then proposed to explain the influence of flame presence on primary atomization.

EXPERIMENTAL SET-UP

The experimental set-up is based on a coaxial injector placed vertically (Fig. 1). Three various liquid tubes may be used with different inner diameter D_l =0.4mm, 1mm and 2mm. In first case, the tube thickness is of 0.3mm, leading to an oxidizer channel inner diameter of D_{gi} = 1mm. For the two other cases, the tube thickness is of 0.5mm, leading to oxidizer channel inner diameter of D_{gi} = 2mm and 3 mm. For oxidizer channel outer tube, three diameters D_{go} are also possible: D_{go} = 3.5mm, 6mm or 8mm.

The coaxial injector is fixed at the bottom of a vertical combustion chamber (Fig. 1). The chamber is made of four identical segments (26 cm inner diameter, 30 cm height). Each individual segment is cooled by a surrounding water jacket. A ceramic fibre layer (alumina) inside the combustion chamber insulates the segments and prevents an excessive cooling of burnt gases leading to condensation. A fifth converging segment is fixed at the top and ensures evacuation of exhaust gases to a chimney. On the first segment, a main window (20 cm x 10 cm) enables direct visualization of the flame whereas two lateral ones may let cross a laser plane. These three windows are made by fused silica. A great care was also taken of the segments' tightness, using ceramic seals, so that no external air intake was possible in the combustion chamber.

Oxidizer and liquid flow rates are monitored using mass flow controllers (BRONKHORST L30 and Elflow). All flows are computer-controlled: in particular it is possible to enter atomization parameters such as momentum flux ratio J or gas flow Reynolds number Re_g as inlet operating conditions. Ethanol flows from a tank pressurized with argon.

The flame is imaged by a CCD camera (PULNIX) through an interferential filter (λ=429.5nm, $\Delta\lambda$=8nm). The filter is centered on the emission band of CH* free radical: CH* corresponds to the excited state (A2Δ) of CH radical and its chemiluminescence is considered to be a good representative of heat release rate [9].

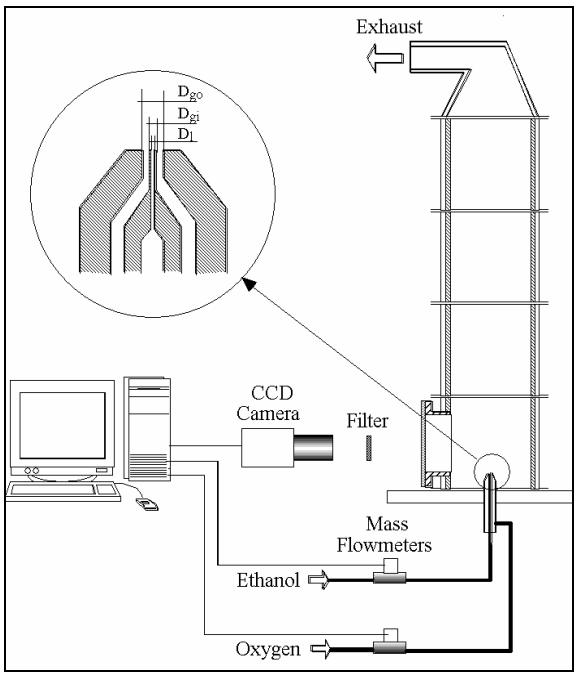

Fig. 1: Description of pilot bench and coaxial injector

Spray evolution is followed by laser tomography, technology which consists in visualizing plane laser light diffused by liquid structures. For that, choosing a wavelength different from natural flame emission is required. As flame emission is very weak in red, He-Ne laser with a power of 30mW has been selected (λ=429.5nm). Thanks to low focal length lens positioned just after the laser outlet (see Fig. 2), we could obtain a 1mm wide and 9cm high laser plane crossing the first combustion chamber module. This laser plane is too wide to distinguish liquid jet from dense spray in case of smallest liquid jet diameter (D_l=0.4mm). Consequently in the following paragraphs, break-up length measurements will be only available for D_l=1mm and D_l=2mm.

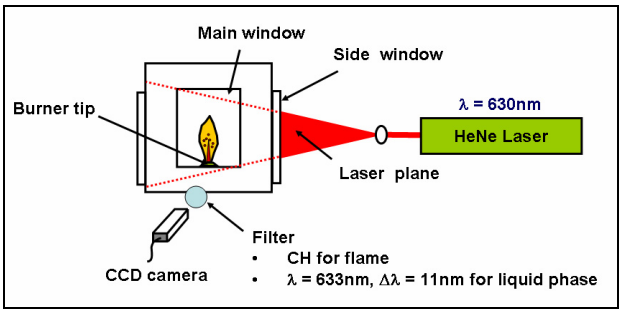

Fig. 2: Diagnostics used for flame and liquid phase visualization

To visualize the light diffused by the liquid flow, the same CCD camera has been used, but with a filter centred on laser beam emission (λ=633nm, $\Delta\lambda$=11nm). So we may have access successively to flame front and spray structure, only by changing filter type. Keeping all the other parameters constant makes easier the comparison of spray position with reaction zone on instantaneous and average pictures (see Fig. 3 for example). Note that in both cases, image resolution is 50 pixel / cm.

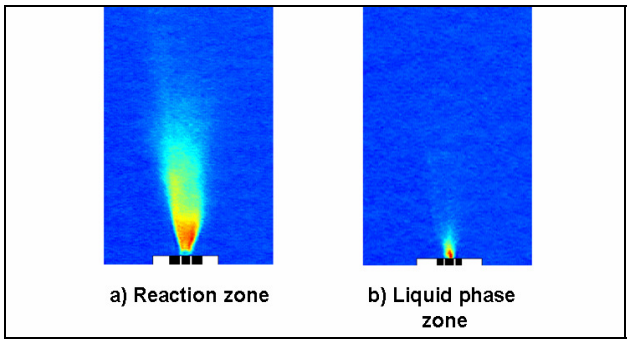

Fig. 3: Instantaneous pictures obtained for reaction and liquid phase zones (D_l =2mm, D_{gi} = 3mm, D_{go}=8mm, U_l = 0.2m/s, U_g = 95m/s)

Whereas atomizing modes are identified thanks to instantaneous pictures, the calculation of average pictures enables to distinguish liquid jet from droplets spray and calculate break-up length in presence of flame. But for that we have to choose an adapted grey levels threshold above which we assess it is no more liquid jet but droplets spray. To help us in the choice of this value, several experiments have been achieved in cold spray conditions to determine the evolution of measured break-up length as a function of threshold. The comparison of this curve with the data measured by shadowgraphy in cold spray conditions (see [2]) enables to get the most suitable threshold. Such a calibration method gives 5% of standard deviation on measured break-up length for almost cases, except for denser atomizing modes for which deviation may reach 10%.

EXPERIMENTAL RESULTS

Among primary atomization properties, we have essentially determined atomising modes and break-up length.

Atomization modes

For atomization modes, the nine geometries have been studied and for each configuration, firing rate and oxidant flow have been modified. The two relevant parameters for atomization modes J and Re_g vary according to a large range: $2000 < Re_g < 50000$ and $0.05 < J < 500$.

Fig. 4 shows some examples of liquid phase instantaneous views obtained for various operating conditions. In presence of flame, the same atomising modes are observed as for cold spray conditions: Rayleigh, membrane type, fiber type and superpulsating.

On Fig. 5, we have reported the observed atomization modes in presence of flame as a function of momentum flux ratio J and gas Reynolds number Re_g . We see that J and Re_g still seem the relevant parameters to classify atomizing modes. However the limits defined in cold spray conditions between the various regimes do not seem valid anymore. In presence of flame, Rayleigh mode appears on a large domain, even for $J > J_r$. Conversely, superpulsating mode becomes very rare, except for values bigger than 300. Globally, Fig. 5 shows that J and Re_g values ensuring an efficient atomization (i.e; fiber and superpulsating modes) are higher in presence of flame than in cold spray conditions. Liquid jet seems stabilized by flame presence.

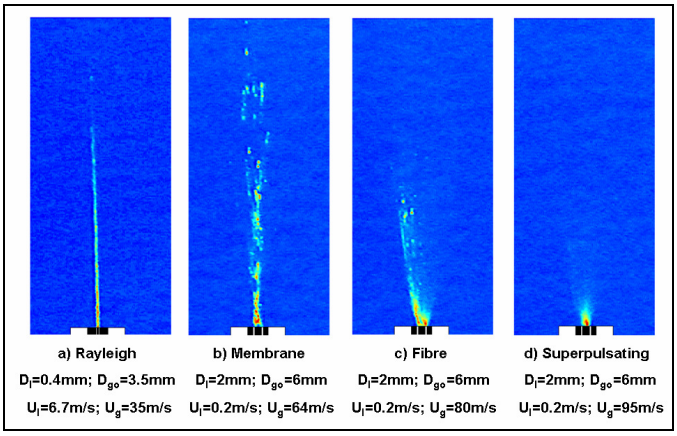

Fig. 4: Identification of atomization modes in presence of flame

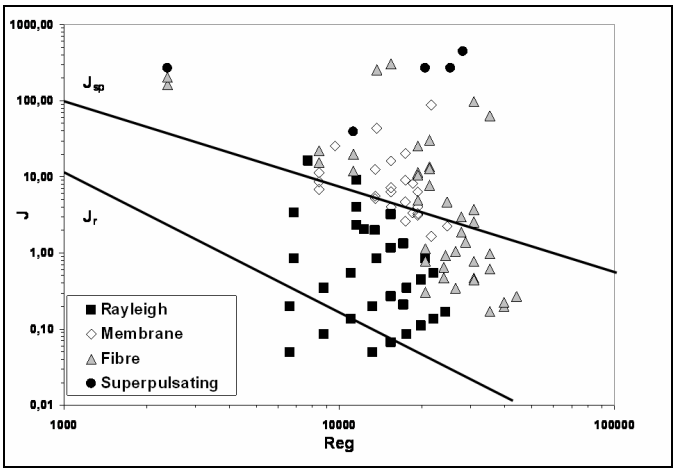

Fig. 5: Classification of atomization modes in presence of flame

Break-up length

For break-up length, only six geometries have been retained. Indeed we have seen that laser plane is too wide for the smallest liquid jet diameter.

Fig. 6 shows break-up length measurements as a function of J, parameter which was relevant in cold spray conditions. We have also reported on Fig. 6 the correlation linking break-up length and J found for cold spray conditions (see Eq. (5)).

Fig. 6 puts into evidence that even in presence of oxy flame, J remains a relevant parameter to quantify break-up length. In particular, modifying the diameter of annular gas flow does not affect liquid cone length. If noting L_b^* the break-up length in presence of oxy flame, we obtain the following relationship:

$$\frac{L_b^*}{D_l} = \frac{60}{\sqrt{J}}. \qquad (6)$$

The exponent found here for J (-0.5) is not same as in cold spray conditions (-0.33) but it is equivalent to the one given by analytical stability models (see for instance [10]). Moreover, the order of magnitude is not the same: break-up length is much more important in presence of flame than in cold spray conditions. The conclusion is the same as the one

resulting from atomizing modes observation: liquid jet seems stabilised by the flame.

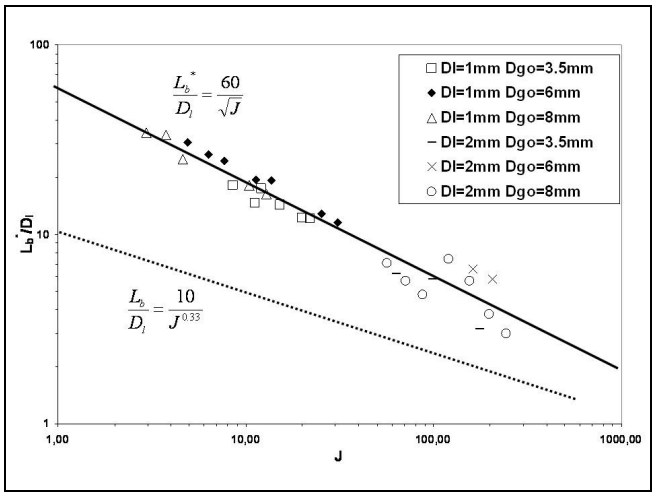

Fig. 6: Evolution of break-up length as a function of J in presence of flame

ANALYTICAL MODEL

The change of atomization properties described previously may be due to a modification of the flow close to the liquid jet. Fig. 7 shows how the flame attached to the nozzle is likely to limit the influence of annular gas flow. Between flame and liquid jet, there is mainly a mixture of vaporised ethanol and burnt gases. Consequently, in the parameters taking into account the velocity of gases useful for atomization, we will not consider oxygen velocity but an effective velocity U_g^* of vaporised ethanol – burnt gases mixture. The physical properties of this mixture (density ρ_g^*, dynamic viscosity μ_g^*, thermal conductivity k_g^*, specific heat capacity $C_{p,g}^*$) are taken at a reference temperature T_{ref} defined by the following equation:

$$T_{ref} = \frac{1}{3}T_{comb} + \frac{2}{3}T_{amb}. \qquad (7)$$

Moreover, vorticity thickness δ is also modified by flame presence. In cold spray conditions, δ is close to the boundary layer thickness in annular gas flow. In presence of flame, the velocity gradient close to the liquid jet is supposed due to vaporized ethanol – burnt gases mixture. For a first approximation, we suppose that this mixture occupies the ring delimited by liquid jet on one hand and oxygen flow on the other hand. In the following paragraphs, in presence of flame, we consider then a vorticity thickness δ^*:

$$\delta^* = \frac{D_{gi} - D_l}{2}. \qquad (8)$$

To see if standard analytical models are suitable in presence of a flame, the velocity U_g^* of burnt gases – vaporized ethanol mixture has first to be calculated.

The mass flow rate of this mixture m_{mix} may be expressed as a function of vaporized ethanol mass flow rate m_{vap}. If considering x the amount of vaporized ethanol which reacts and κ the ratio of products molar mass with fuel molar mass in stoechiometric conditions, it comes:

$$m_{mix} = \kappa x m_{vap} + (1-x)m_{vap}, \qquad (9)$$

the first term corresponding to the mass flow rate of burnt gases and the second one to ethanol which has not reacted.

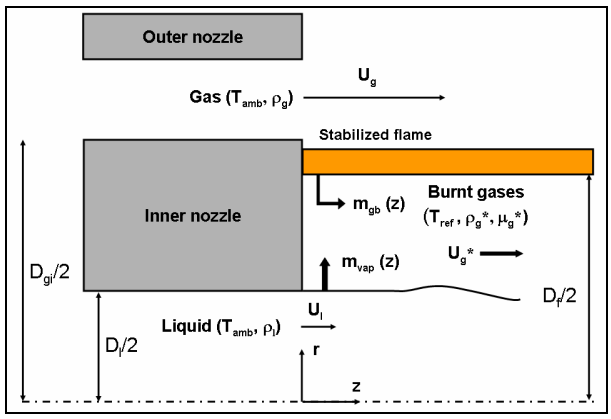

Fig. 7: Modification of flow structure due to presence of flame front

Eq. (9) may be simplified:

$$m_{mix} = \left[1 + x(\kappa - 1)\right]m_{vap}, \qquad (10)$$

Note that κ only depends on reactants molar masses. For ethanol – oxygen reaction, in stoechiometric conditions:

$$\kappa_{C2H5OH/O2} = \frac{2M_{CO2} + 3M_{H2O}}{M_{C2H5OH}} = 3.1 \qquad (11)$$

To assess vaporized mass flow rate m_{vap} in Eq. (10), we may use the results of [11] reported by [12] about plane liquid surfaces burning in co-flowing convective flows, showing the importance of boundary layer development in vaporized liquid amount since it forces gradients in longitudinal and transverse directions. In particular, [11] has expressed the vaporized liquid fuel flow rate per surface unit G_{vap} as follows, supposing Schmidt number equal to 1:

$$G_{vap}(z) = \frac{k_g^*}{C_{pg}^*}\frac{\mathrm{Re}_{\delta(z)}^{0.5}}{\sqrt{2}\,\delta(z)}\frac{\ln(1+B)}{2.6B^{0.15}}, \qquad (12)$$

with z the distance from the edge of liquid surface (see Fig. 8), k_g^* the thermal conductivity of the gas taken at reference temperature T_{ref}, $C_{p,g}^*$ its specific heat capacity, $\mathrm{Re}_{\delta(z)}$ the Reynolds number linked to vorticity thickness and B the transfer constant defined by [13] for the considered fuel – oxidant couple.

Eq. (12) may be adapted to coaxial injector configuration, supposing a constant vorticity thickness defined by Eq. (8) and positioning the problem in liquid jet referential. Vaporized liquid fuel flow rate per surface unit becomes:

$$G_{vap} = \frac{k_g^*}{C_{pg}^*}\frac{1}{\sqrt{D_{gi} - D_l}}\sqrt{\frac{\rho_g^*(U_g - U_l)}{\mu_g^*}}\frac{\ln(1+B)}{2.6B^{0.15}}. \qquad (13)$$

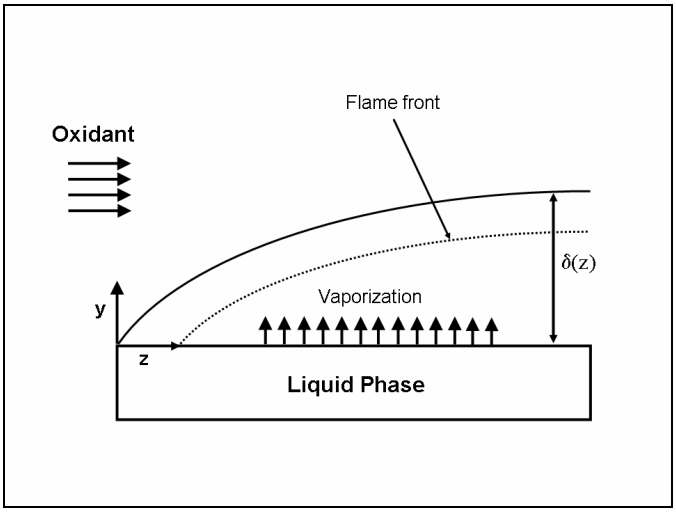

Fig. 8: Combustion of plane liquid surface in a co-flowing oxidant flow ([12])

Eq. (13) shows that G_{vap} remains constant along longitudinal direction. However, the amount of burnt gases – vaporized ethanol accumulates when z increases. Consequently, to calculate m_{mix} at a certain distance z from injection, we have to consider the total amount of vaporized ethanol in a liquid jet cylinder located between 0 and z. It comes then:

$$m_{mix} = \left[1 + x(\kappa - 1)\right] \int_0^z \pi \, D_l G_{vap}(u) du \,. \qquad (14)$$

Dividing m_{mix} by density ρ_g^* and by the section of mixture flow, it comes for atomization velocity:

$$U_g^*(z) = \left[1 + x(\kappa - 1)\right] \frac{4 D_l G_{vap}}{\rho_g^* (D_{gi}^2 - D_l^2)} z \,, \qquad (15)$$

and if replacing G_{vap} by Eq. (13) and considering that usually $U_g >> U_l$:

$$U_g^*(z) = 1.5 X A \alpha_g^* \sqrt{\frac{U_g}{\nu_g^*}} z \,, \qquad (16)$$

with α_g^* and ν_g^* respectively thermal diffusivity and kinematic viscosity of the mixture considered at T_{ref}, X a constant depending on fuel – oxidant flow and vaporization rate :

$$X = \left[1 + x(\kappa - 1)\right] \frac{\ln(1 + B)}{B^{0.15}} \,, \qquad (17)$$

and A a geometric factor :

$$A = \frac{D_l}{\sqrt{D_{gi} - D_l} \, (D_{gi}^2 - D_l^2)} \,. \qquad (18)$$

To get an idea of orders of magnitude introduced by this new approach, we have used Eq. (15) to assess atomization velocity U_g^* for the following operating conditions: D_l = 1mm, D_{go} = 6mm, U_l = 0.7m s^{-1} and U_g = 78m s^{-1}. Fig. (9) shows the result of this calculation for x = 0 (no reaction of vaporized ethanol) and for x = 1 (all the vaporized fuel has burnt). We notice that mixture velocity is more important when all the vaporized fuel is consumed (x=1), which may be explained by the higher mass of combustion products than fuel one. But even for x = 1, this is only for z = 10D_l that mixture velocity becomes close to oxidant one. This may then explain why primary atomization efficiency is weaker when flame is attached to injector tip than in cold spray conditions.

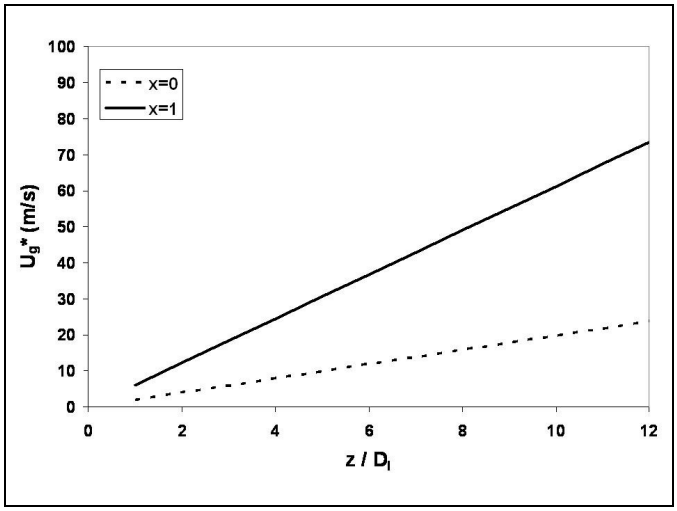

Fig. 9: Evolution of atomization velocity for vaporized fuel – burnt gases mixture as a function of distance from injection (D_l = 1mm, D_{go} = 6mm, U_l = 0.7m s^{-1} and U_g = 78m s^{-1})

We have also checked if standard analytical models for primary atomization (as detailed by [10] for instance) were still suitable, taking into account this new value for atomising gas velocity. In particular we have recalculated in presence of flame a break-up length L_b^* and expressed it as function of momentum flux ratio J. For that, as U_g^* is no more constant and depends on z, we have first to consider a mean velocity $\overline{U}_g^*$ seen by liquid jet during primary atomization step, that is to say for z varying between 0 and L_b^*:

$$\overline{U}_g^* = \frac{\int_0^{L_b^*} U_g^*(z) dz}{L_b^*} \,. \qquad (19)$$

If replacing $U_g^*(z)$ with Eq. (15), it comes:

$$\overline{U}_g^* = 0.75 X A \alpha_g^* \sqrt{\frac{U_g}{\nu_g^*}} L_b^* \,. \qquad (20)$$

The second expression linking L_b^* and $\overline{U}_g^*$ may be given by one of the analytical models existing for cold spray conditions, for instance the relationship of [10]:

$$\frac{L_b^*}{D_l} = \frac{6}{\sqrt{\frac{\rho_g^* U_g^{*2}}{\rho_l U_l^2}}} \,. \qquad (21)$$

The resolution of this system of two equations with two variables gives for L_b^* and U_g^*:

$$\frac{L_b^*}{D_l} = \sqrt{\frac{8}{X}} \frac{1}{J^{0.25}} \left(\frac{\rho_g}{\rho_g^*} \right)^{0.25} \left(\frac{U_g (D_{gi} - D_l)}{\nu_g^*} \right)^{0.25} \sqrt{\mathrm{Pr}_g^*} \frac{\sqrt{(D_{gi}^2 - D_l^2)}}{D_l}, \quad (22)$$

$$U_g^* = 2.1 \sqrt{X} \frac{1}{J^{0.25}} \left(\frac{\rho_g}{\rho_g^*} \right)^{0.25} \left(\frac{\nu_g^*}{U_g (D_{gi} - D_l)} \right)^{0.25} \frac{1}{\sqrt{\mathrm{Pr}_g^*}} \frac{D_l}{\sqrt{(D_{gi}^2 - D_l^2)}} U_g, \quad (23)$$

with Pr_g^* the Prandtl number, ratio of ν_g^* and α_g^* for burnt gases – vaporized ethanol mixture. We have then calculated L_b^* given by Eq. (6) for the experimental data reported on Fig. 6. For that, two cases have been considered: x=0 (no combustion of vaporized ethanol) and for x=1 (all the vaporized fuel has been burnt). Fig. 10 compares these calculated values with experimental data.

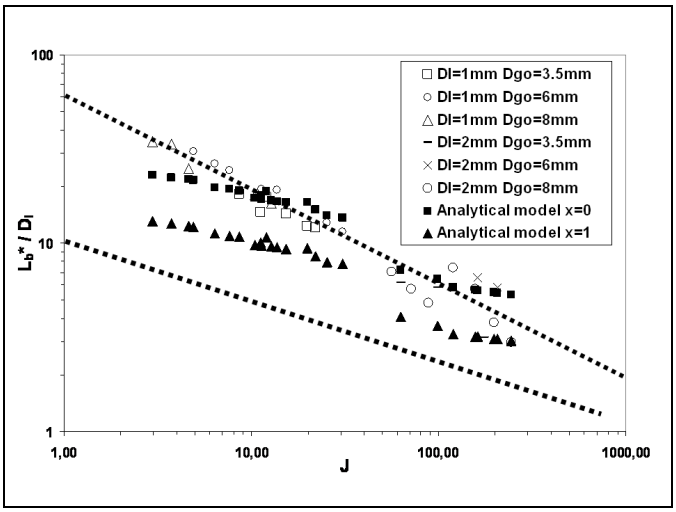

Fig. 10: Evolution of break-up length in presence of a flame: comparison with the proposed analytical model

Whatever the mixture composition and x value, analytical break-up length is confirmed being higher than data obtained in cold spray conditions. Moreover, the values obtained for x=0 enable to predict more accurately the break-up length in presence of flame: only a small amount of vaporized fuel would be really burnt during primary atomization. This would be essentially vaporized ethanol which would cause the destabilization of liquid jet.

Certainly some reserves might be raised up against this model. First Eq. (22) does not give the same exponent for J as deduced experimentally (-0.25 vs -0.5). Moreover analytical model suggests that other parameters than J have to be considered for break-up length variation, especially gas velocity U_g or inner tube thickness of the injector, which was not observed experimentally.

But despite these reserves, this analytical model - emphasizing the relevance of vaporized ethanol velocity - gives the right order of magnitude for break-up length. Moreover expressions giving break-up length are still valid if considering no more J but J*, the momentum flux ratio between burnt gases – vaporized ethanol mixture and liquid flows.

CONCLUSIONS

In the present study, we have investigated the influence of flame on primary atomization in oxy- liquid ethanol flames by using a coaxial air-assisted injector positioned in a vertical combustion chamber. Nine geometries were available for this study enabling to cover a large range of liquid and gas velocities for given firing rate and stoechiometry. Flame structure has been observed through CH emission whereas liquid phase has been put into evidence by laser tomography.

The classification of atomizing modes in presence of flame has shown that momentum flux ratio J and gas Reynolds number Re_g were still the relevant parameters; however the limits defined in cold spray conditions between the various regimes did not seem valid anymore. In particular the values of J and Re_g for which atomization was efficient enough were much higher in presence of flame. Break-up length measurements have enabled to arrive to the same conclusion: in presence of flame, break-up length was two to six times as important as in cold spray conditions.

These observations have been explained by the position of reaction zone on the coaxial geometries we have used. Indeed, as flame is stabilized on the inner tube located between ethanol and oxygen flows, and due to very low reaction time for oxy combustion, we have assumed that there was no oxygen between the flame front and the liquid core. Consequently this is not the annular gas flow which causes primary atomization but a mixture of burnt gases and vaporized ethanol. New length and velocity scales have then been chosen: for length scale, the inner tube thickness and for velocity scale, we consider the average velocity of the burnt gases – vaporized ethanol mixture before the break-up of the liquid core. We show that this average velocity depends on x the proportion of vaporized ethanol actually burnt, on inner nozzle geometry and on annular gas flow physical properties and velocity. Thanks to this model, it is possible to assess an analytical break-up length close to experimental data.

This demonstrates the strong coupling between atomisation and combustion in oxy – liquid fuel flame. Whereas for air firing, flame influence is limited to quicker vaporization of droplets, this study confirms here the modification of primary atomization properties due to a change of local aerodynamics close to injections.

NOMENCLATURE

Symbol	Quantity	SI Unit
A	Geometric factor (see Eq. (18))	
α_g^*	Thermal diffusivity	$m^2\ s^{-1}$
B	Transfer constant	
$C_{p,g}^*$	Specific heat capacity of burnt gases – vaporized ethanol mixture	$J\ kg^{-1}\ K^{-1}$
D_{gi}	External diameter of central tube	m
D_{go}	External nozzle diameter	m
D_l	Liquid jet diameter	m
δ	Vorticity thickness in cold spray conditions	m
δ^*	Vorticity thickness in presence of flame	m
G_{vap}	Vaporized liquid fuel flow rate per surface unit	$kg\ s^{-1}\ m^{-2}$
J	Momentum flux ratio between gas	

	and liquid flows	
J^*	Momentum flux ratio between burnt gases – vaporized ethanol mixture and liquid flows	
k_g^*	Thermal conductivity of burnt gases – vaporized ethanol mixture	$W\ m^{-1}\ K^{-1}$
κ	Ratio of combustion products molar mass with fuel molar mass in stoechiometric conditions	
L_b	Break-up length	m
L_b^*	Break-up length in presence of flame	m
m_{mix}	Mass flow rate of burnt gases – vaporized ethanol mixture	$kg\ s^{-1}$
m_{vap}	Mass flow rate of vaporized ethanol flow	$kg\ s^{-1}$
M	Molar mass	$g\ mol^{-1}$
μ_g^*	Dynamic viscosity of burnt gases – vaporized ethanol mixture	Pa s
ν_g^*	Kinematic viscosity of burnt gases – vaporized ethanol mixture	$m^2\ s^{-1}$
Pr_g^*	Prandtl number for burnt gases – vaporized ethanol mixture considered at T_{ref}	
Re	Reynolds number	
ρ_g^*	Density of burnt gases – vaporized ethanol mixture	$kg\ m^{-3}$
T_{amb}	Ambient temperature	K
T_{comb}	Adiabatic temperature of reaction	K
T_{ref}	Reference temperature of burnt gases – vaporized ethanol mixture (see Eq. (7))	K
U_g	Atomization gas velocity	$m\ s^{-1}$
U_g^*	Atomization velocity in presence of flame	$m\ s^{-1}$
U_l	Liquid fuel velocity	$m\ s^{-1}$
X	Constant typical of fuel – oxidant couple (see Eq. (17))	
z	Longitudinal direction – Distance from the injection	m

REFERENCES

[1] B. Lewis and G. Von Elbe, Combustion, flames and explosions of gases, New York: Academic Press, 1951.

[2] B. Leroux, O. Delabroy and F. Lacas, Experimental study of coaxial atomizers scaling. Part I : dense core zone, *Atomization and Sprays,* vol. 17, pp. 381-407, 2007.

[3] Z. Farago and N. Chigier, Morphological classification of disintegration of round liquid jets in coaxial air stream, *Atomization and Sprays,* vol. 2, pp. 137-153, 1992.

[4] J.C. Lasheras, E. Villermaux and E.J. Hopfinger, Break-up and atomization of a round water jet by a high-speed annular air jet, *J. Fluid Mech.,* vol. 357, pp. 351-379, 1998.

[5] C.P. Mao, G. Wang and N. Chigier, An experimental study of air-assist atomizer spray flames, *Proc. of Twenty-first Symposium (International) on Combustion,* pp. 665-673, 1986.

[6] V. McDonell, M. Adchi and G. Samuelsen, Structure of reacting and non reacting nonswirling, air-assisted sprays, *Atomization and Sprays.,* vol. 3, pp. 389-436, 1993.

[7] A. Gupta, C. Presser, J. Hodges and C. Avedisian, Role of combustion on droplet transport in pressure-atomized spray flames, *Journal of Propulsion and Power,* vol. 12, No. 3, pp. 543-553, 1996.

[8] F. Lacas, B. Leroux and N. Darabiha, Experimental study of air dilution in oxy liquid fuel flames, *Proc. of Thirtieth Symposium (International) on Combustion,* pp. 2037-2045, 2004.

[9] N. Docquier, S. Belhalfaoui, F. Lacas, N. Darabiha, and J. C. Rolon, Experimental and numerical study of chemiluminescence in methane/air high pressure flames for active control applications, *Proc. of Twenty-eight Symposium (International) on Combustion,* pp. 1765-1774, 2000.

[10] E. Villermaux, Mixing and spray formation in coaxial jets, *Journal of Propulsion and Power,* vol. 14, No. 5, pp. 807-817, 1998.

[11] H. Emmons, The film combustion of liquid fuel, *Z. Angew Math. Mech.,* vol. 36, pp. 60-71, 1956.

[12] I. Glassman, Combustion, 3rd Edition, Academic Press, 1996.

[13] D. Spalding, The combustion of liquid fuels, *Proc. of Fourth Symposium (International) on Combustion,* pp. 847-864, 1953.